

# Direct signaling by the BMP type II receptor via the cytoskeletal regulator LIMK1

Victoria C. Foletta,<sup>1</sup> Mei Ann Lim,<sup>1</sup> Juliana Soosairajah,<sup>1</sup> April P. Kelly,<sup>1</sup> Edouard G. Stanley,<sup>1</sup> Mark Shannon,<sup>1</sup> Wei He,<sup>2</sup> Supratik Das,<sup>2</sup> Joan Massagué,<sup>2</sup> and Ora Bernard<sup>1</sup>

<sup>1</sup>The Walter and Eliza Hall Institute of Medical Research, 1G Royal Parade Parkville, Victoria 3050, Australia

<sup>2</sup>Cell Biology Program and Howard Hughes Medical Institute, Memorial Sloan-Kettering Cancer Center, New York, NY 10021

**B**one morphogenetic proteins (BMPs) regulate multiple cellular processes, including cell differentiation and migration. Their signals are transduced by the kinase receptors BMPR-I and BMPR-II, leading to Smad transcription factor activation via BMPR-I. LIM kinase (LIMK) 1 is a key regulator of actin dynamics as it phosphorylates and inactivates cofilin, an actin depolymerizing factor. During a search for LIMK1-interacting proteins, we isolated clones encompassing the tail region of BMPR-II. Although the BMPR-II tail is not involved in BMP signaling via Smad

proteins, mutations truncating this domain are present in patients with primary pulmonary hypertension (PPH). Further analysis revealed that the interaction between LIMK1 and BMPR-II inhibited LIMK1's ability to phosphorylate cofilin, which could then be alleviated by addition of BMP4. A BMPR-II mutant containing the smallest COOH-terminal truncation described in PPH failed to bind or inhibit LIMK1. This study identifies the first function of the BMPR-II tail domain and suggests that the deregulation of actin dynamics may contribute to the etiology of PPH.

## Introduction

LIM kinase 1 (LIMK1) regulates actin dynamics by phosphorylating cofilin on serine 3, rendering it inactive, as phosphorylated cofilin is unable to bind actin and mediate actin depolymerization (Arber et al., 1998; Yang et al., 1998). In turn, LIMK1 is activated after phosphorylation by two protein kinases, p21-activated kinases (PAKs) and Rho-associated kinase (ROCK) (Edwards et al., 1999; Maekawa et al., 1999; Dan et al., 2001), effectors of the small GTPases Rac, Cdc42, and Rho. In addition to its ki-

nase domain, LIMK1 contains two LIM domains and one PDZ domain. These domains mediate protein-protein interactions and are suggested to regulate the activity of LIMK1, as deletion mutants lacking these domains show increased LIMK1 activity (Arber et al., 1998). Previous yeast two-hybrid and mammalian cell interaction analyses have revealed that LIMK1 interacts with its LIM domains with at least two other non-LIM proteins, PKC (Kuroda et al., 1996) and the cytoplasmic domain of the transmembrane ligand neuregulin (Wang et al., 1998). However, no function was assigned to these interactions. Recently, it was identified that both LIMK1 and cofilin interact with the scaffolding protein 14-3-3  $\zeta$  (Gohla and Bokoch, 2002; Birkenfeld et al., 2003). The 14-3-3  $\zeta$  protein also binds to phospho-cofilin and may cooperate with LIMK1 in maintaining phospho-cofilin levels (Gohla and Bokoch, 2002).

Bone morphogenetic protein receptors (BMPRs) are transmembrane serine/threonine protein kinases that belong to the TGF $\beta$  family of receptors and consist of type I and type II proteins. Ligand binding leads the type II BMPR (BMPR-II) to phosphorylate and activate the type I receptors, BMPR-IA (also known as ALK3) and BMPR-IB (ALK6).

V.C. Foletta and M.A. Lim contributed equally to this work.

Address correspondence to Ora Bernard, The Walter and Eliza Hall Institute of Medical Research, 1G Royal Parade Parkville, Victoria 3050, Australia. Tel.: 61-3-93452494. Fax: 61-3-93470852. email: bernard@wehi.edu.au

V.C. Foletta's present address is Metabolic Research Unit, School of Health Sciences, Deakin University, Geelong Victoria 3217, Australia.

M.A. Lim's present address is Department of Pharmacology, University of Texas Health Science Center at San Antonio, San Antonio, TX 78229.

A.P. Kelly's present address is Division of Cell Biology and Immunology, School of Life Sciences, Dundee DD1 5EH, UK.

E.G. Stanley's present address is Monash Institute for Reproduction and Development, Monash Medical Centre, Victoria 3168, Australia.

M. Shannon's present address is Peter MacCallum Cancer Institute, Victoria 3002, Australia.

S. Das's present address is Department of Physiology, University of Connecticut Health Center, Farmington, CT 06030.

Key words: LIM kinase 1; BMPR-II; cytoskeleton; F-actin; cofilin

Abbreviations used in this paper: BMP, bone morphogenetic protein; BMPR, BMP receptor; LAP, LIMK1-associated protein; LIMK, LIM kinase; PAK, p21-activated kinase; PPH, primary pulmonary hypertension; ROCK, Rho-associated kinase.

BMPR-I, in turn, phosphorylates Smad proteins, causing their activation and translocation to the nucleus where they regulate the transcription of BMP-responsive genes (Shi and Massague, 2003).

The only function of the TGF $\beta$  family type II receptors known to date is the phosphorylation of type I receptors. Unlike other TGF $\beta$  type II receptors, however, BMPR-II has a large cytoplasmic tail of  $\sim$ 600 amino acids COOH terminal to the kinase domain. This domain is present in the most abundant splice form of BMPR-II, and a similar domain (albeit of very different amino acid sequence) is also present in the *Drosophila* BMPR-II (Aberle et al., 2002; Allan et al., 2003). To date, no function has been assigned to this domain, as it is not required for BMP signaling through the Smad pathway (Wieser et al., 1993; Nishihara et al., 2002).

Mutations within BMPR-II are implicated in the rare autosomal dominant disorder primary pulmonary hypertension (PPH), which is characterized by the proliferation of pulmonary artery smooth muscle and endothelial cells, resulting in occlusion of pulmonary vessels and increased blood pressure followed by heart failure (Morrell et al., 2001). Many of the *BMPRII* mutations identified in PPH occur downstream of the kinase domain and are either frameshift or nonsense mutations that are predicted to truncate the tail domain (Lane et al., 2000; Thomson et al., 2000; Machado et al., 2001). These observations suggest that the tail may play an important role in the regulation of pulmonary artery wall homeostasis.

Here, we demonstrate that LIMK1 interacts specifically with the tail of BMPR-II via its LIM domains and that this interaction results in the down-regulation of LIMK1 activity. We show that BMP4 ligand stimulation alleviates this down-regulation, resulting in increased levels of phosphocofilin and changes to the actin cytoskeleton and subcellular localization of LIMK1. Furthermore, a mutation in the BMPR-II mimicking the most COOH-terminal mutation in PPH reduces the ability of BMPR-II to bind and inhibit LIMK1, raising the possibility that LIMK1 is involved in the etiology of PPH.

## Results

### LIMK1 interacts with the tail of BMPR-II

To identify new molecules that regulate LIMK1 activity, we conducted yeast two-hybrid screens (Fields and Song, 1989) to isolate LIMK1-associated proteins (LAPs). After screening of mouse embryonic and human brain cDNA libraries using full-length LIMK1 fused to the GAL4 DNA binding domain as bait, two clones from each library interacted strongly with LIMK1 but did not interact with two negative control baits (Jun and Lck) or empty vector. These four clones were picked for further analysis as they demonstrated the greatest  $\beta$ -galactosidase activity and hence the strength of interaction in this particular assay system. Sequence analysis of these LAPs (mLAP16, mLAP22, hLAP15, and hLAP41) revealed that they all contained cDNA inserts corresponding to a region within the cytoplasmic tail of BMPR-II (Fig. 1 A). The interaction between LIMK1 and the tail of BMPR-II was confirmed in mammalian cells. The cDNAs of the three LAPs (mLAP16, hLAP15, and hLAP41)

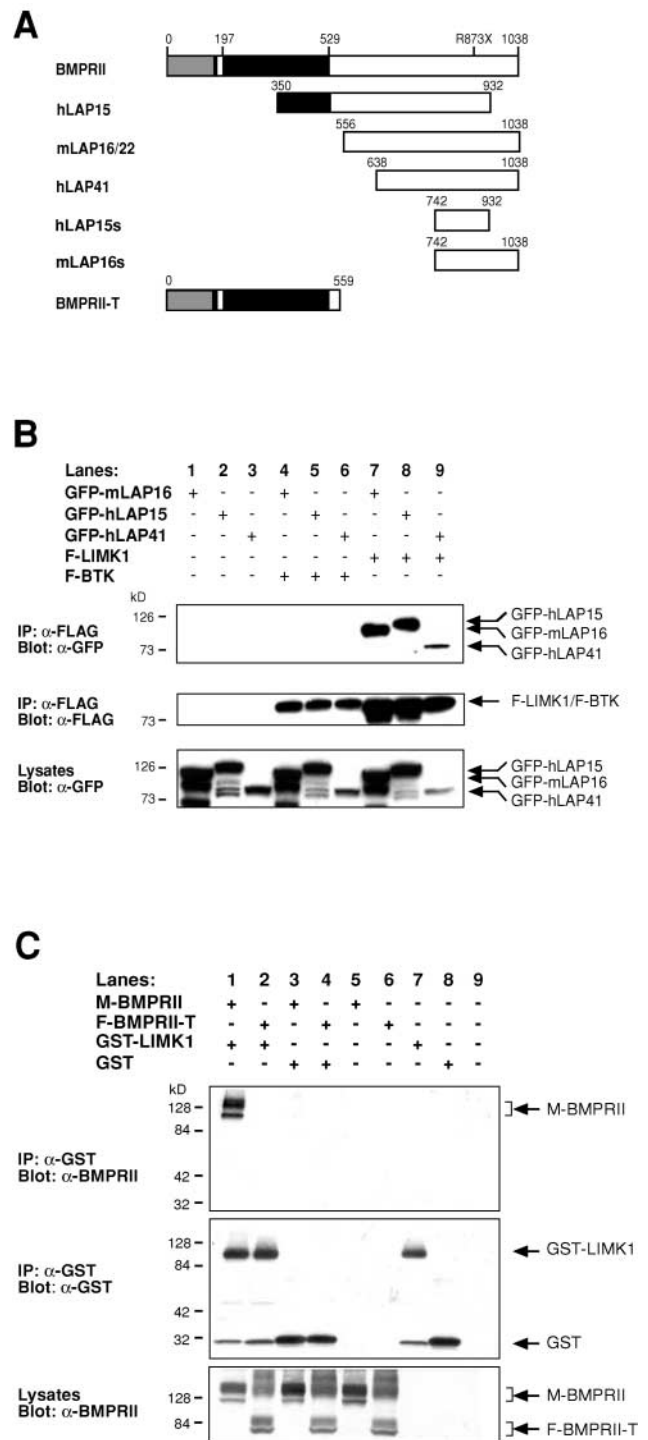


**Figure 1. Immunoprecipitation analyses of overexpressed LIMK1 and its interaction with BMPR-II proteins in COS-7 cells.** (A) Schematic representation of full-length and truncated BMPRII proteins. The extracellular domain (gray), the transmembrane and kinase domains (small and large black areas, respectively), and the cytoplasmic tail (white) are presented. The numbers of the amino acid residues are indicated above each structure as well as the site of the most COOH-terminal mutation currently identified in PPH patients, R873X. (B) Immunoprecipitation and immunoblot analyses of GFP-tagged LAPs interacting with FLAG-tagged LIMK1 (F-LIMK1) but not FLAG-Btk (F-Btk). (C) GST-tagged LIMK1 interaction with full-length myc-tagged BMPR-II (M-BMPRII) or FLAG-tagged truncated BMPR-II (F-BMPRII-T; contains no cytoplasmic tail).

were subcloned into GFP-encoding expression vectors and were coexpressed with either FLAG-tagged LIMK1 or Btk, a cytoplasmic protein kinase unrelated in function to LIMK1, in COS-7 cells. The FLAG-tagged proteins were immunopurified with FLAG M2 beads, and interacting proteins were detected by Western blotting with an anti-GFP antibody (Fig. 1 B). All three LAPs interacted with LIMK1 (lanes 7–9) but not with Btk (lanes 4–6) or with the FLAG beads alone (lanes 1–3).

To determine whether full-length BMPR-II, which normally localizes to the cell membrane as part of a BMPR complex, associates with LIMK1, full-length myc-tagged BMPR-II was coexpressed with either GST or GST–LIMK1 in COS-7 cells. Cell lysates were incubated with glutathione-Sepharose beads, and the bound proteins were analyzed by immunoblotting with an anti-BMPR-II antibody (Fig. 1 C). Full-length BMPR-II was observed to bind to GST–LIMK1 (lane 1) but not to GST (lane 3), suggesting that BMPR-II interacts with LIMK1 in mammalian cells. We also found that the other member of the LIMK family, LIMK2, interacted with full-length BMPR-II when both proteins were overexpressed in COS-7 cells (unpublished data).

Studies by Liu et al. (1995) suggested that BMPR-II existed as two isoforms generated by alternative splicing. These isoforms differed in that one, BMPR-IIs, lacked the long cytoplasmic region identified as LIMK1-interacting domain in our yeast two-hybrid screen. To investigate whether the region required for the interaction between BMPR-II and LIMK1 occurs specifically within the cytoplasmic tail region of BMPR-II, we performed pull-down experiments using a truncated version of BMPR-II, which does not possess the cytoplasmic tail (amino acid residues 1–559; Fig. 1 A). Truncated BMPR-II was unable to bind GST–LIMK1 or GST alone (Fig. 1 C, lanes 2 and 4). These results suggested that only the long form of BMPR-II was able to interact with LIMK1.

### In vivo interaction between endogenous LIMK1 and BMPR-II

It is possible that the interaction between overexpressed BMPR-II and GST–LIMK1 was driven by the large amounts of the proteins produced in the COS cell overexpression system. To address this issue, we sought to determine if the interaction occurred between endogenously expressed proteins in tissue culture cells. Initially, we performed a survey of human and mouse cell lines for expression of LIMK1, BMPR-II, and the alternative spliced protein lacking the cytoplasmic tail, BMPR-IIs (Liu et al., 1995). RNAs encoding the BMPR-IIs were of particular interest because our results implied that cells might be able to modulate the amount of BMPR-II–LIMK1 complex by altering the proportion of BMPR-II to BMPR-IIs. However, Northern blot analysis of most of the cell lines examined, which included human HaCaT keratinocytes, HPL1 lung epithelial cells, HUVEC umbilical cord endothelial cells, WI38 lung fibroblasts, A549 lung carcinoma, HepG2 hepatoma, and mouse NMuMG mammary epithelial cells, C2C12 myoblasts, and NIH3T3 mouse embryo fibroblasts, showed mRNA expression of *BMPRII* and *Limk1* but not *BMPRIIs* (unpublished data). To facilitate

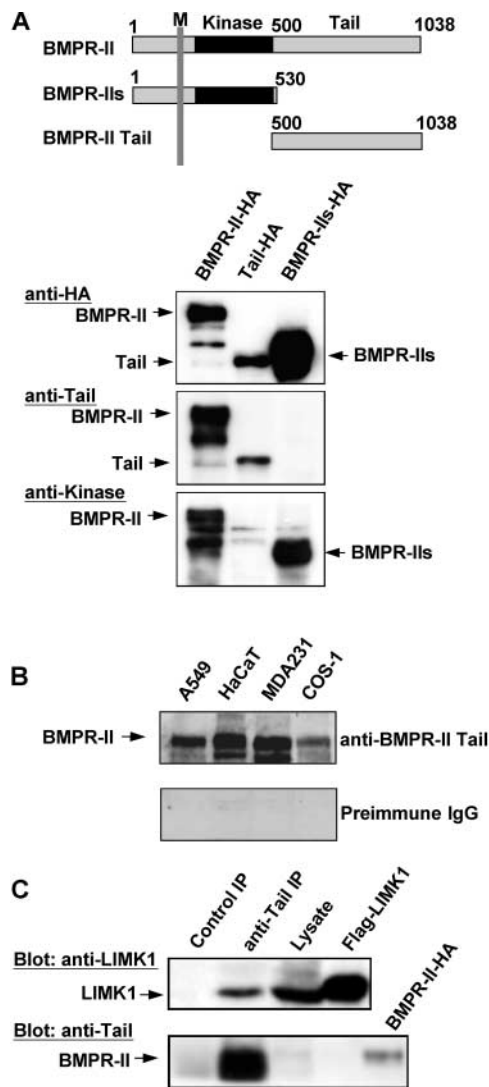


**Figure 2. Interaction between endogenous LIMK1 and BMPR-II.** (A) Schematic representation of BMPR-II, the short alternatively spliced isoform BMPR-IIs and the COOH-terminal tail construct, and recognition of these proteins, expressed in COS-7 cells as HA-tagged constructs, by anti-kinase domain and anti-tail domain antibodies. M, transmembrane region. (B) Recognition of endogenous BMPR-II by anti-BMPR-II-tail antibodies in Western immunoblotting of lysates from the indicated cell lines. (C) Association of endogenous BMPR-II and LIMK1 in NIH3T3 cells. Lysates from NIH3T3 cells were immunoprecipitated with anti-BMPR-II-tail antibodies, and the presence of BMPR-II and LIMK1 in the immunocomplexes was determined by Western immunoblotting with the indicated antibodies. Two percent of the total lysate used for immunoprecipitation was tested by immunoblotting for LIMK1 expression (Lysate). FLAG-tagged LIMK1 and HA-tagged BMPR-II immunoprecipitated from transfected COS-7 cells with antibodies against these epitopes served as marker controls.

the analysis of BMPR-II–LIMK1 interactions, we raised rabbit polyclonal antibodies against the kinase domain and the cytoplasmic tail of BMPR-II domain (Fig. 2 A) in addition to using a mouse monoclonal anti-LIMK1 antibody that recognizes endogenous LIMK1 protein. Western immunoblotting of cell lysates using these antibodies after a survey of selected cell lines revealed that BMPR-II is expressed in all cell lines tested (Fig. 2 B; unpublished data).

NIH3T3 fibroblasts, which express an intermediate level of BMPR-II, also expressed a moderate level of LIMK1 (Fig. 2 C) and were used to investigate the interaction between these two endogenous proteins. Immunoprecipitation of cell lysates with anti-BMPR-II (tail) antibodies followed by Western immunoblotting of these precipitates with mouse anti-LIMK1 monoclonal antibody demonstrated an interaction between endogenous BMPR-II and LIMK1 proteins (Fig. 2 C).

### BMPR-II mapping of the LIMK1 binding region

Having established that the tail of BMPR-II was required for its interaction with LIMK1, we then sought to define the minimal region within the tail required for this interaction.

The sequences responsible for the LIMK1-BMPR-II interaction were further defined by creating myc-tagged BMPR-II tail deletion constructs. Plasmids encoding truncated versions of hLAP15 (hLAP15s, amino acids 742-932) and mLAP16 (mLAP16s, amino acids 742-1038) (Fig. 1 A) were cotransfected with constructs encoding either GST-LIMK1 or GST alone. After affinity purification with glutathione-Sepharose beads, proteins that copurified with the GST fusion proteins were detected using an anti-myc antibody (Fig. 3 A). Both mLAP16s and mLAP15s interacted with GST-LIMK1 but not with GST, indicating that the minimal region required for BMPR-II interaction with LIMK1 is contained within a 190-amino acid region located COOH terminal to the BMPR-II kinase domain.

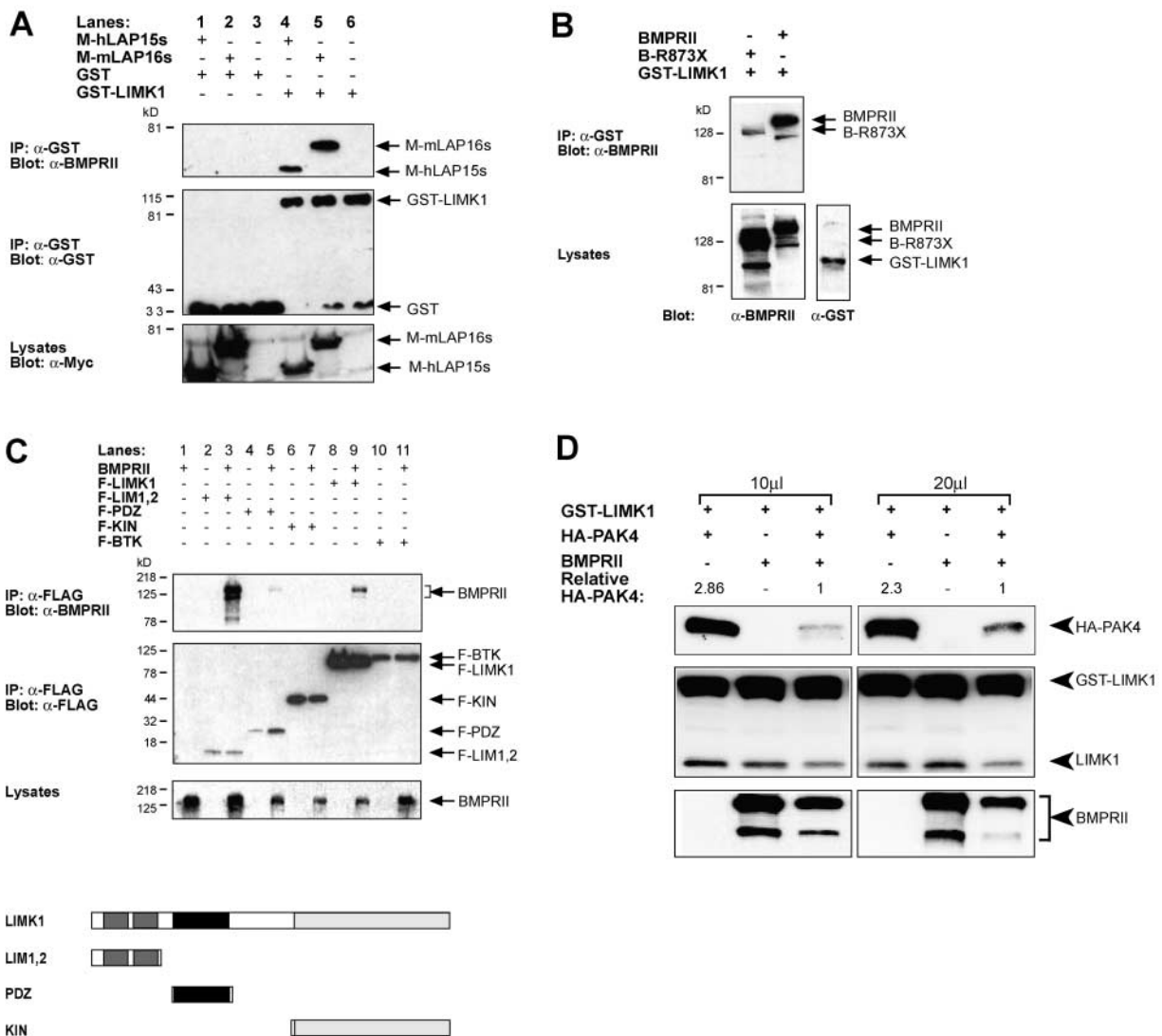


**Figure 3. Analysis of LIMK1 and BMPR-II interaction.** (A) GST-LIMK1 interaction with myc-tagged LAP proteins (M-hLAP15s and M-mLAP16s); isolated regions of the cytoplasmic tail of BMPR-II. (B) GST-LIMK1 interaction with wild-type, untagged BMPR-II and mutated BMPR-II (B-R873X) containing a COOH-terminal mutation (see Fig. 1 A). (C) FLAG-tagged LIM and PDZ domains of LIMK1 (F-LIM1,2 and F-PDZ) and full-length F-LIMK1, but not FLAG-tagged LIMK1 kinase domain (F-KIN) or F-Btk, interact with full-length BMPR-II. A schematic diagram of the LIMK1 domains is represented below the panels. The LIM domains (dark gray), PDZ domain (black), and kinase region (light gray) are indicated. (D) Association of two different amounts (10 and 20  $\mu$ l) of GST-LIMK1 bound to glutathione-Sepharose beads with HA-PAK4 (lanes 1 and 4), BMPR-II (lanes 2 and 5), and both PAK4 and BMPR-II (lanes 3 and 6). Numbers above the blots indicate the fold change in HA-PAK4's ability to bind GST-LIMK1 in the presence and absence of overexpressed BMPR-II.

### BMPR-II mutation that mimics the most COOH-terminal mutation in PPH affects binding to LIMK1

The region of 190 amino acids in the tail of BMPR-II encompasses sequences that are affected by mutations associated with PPH (Machado et al., 2001). To test whether such mutations influence the binding of BMPR-II to LIMK1, we created a BMPR expression construct encoding a BMPR-II bearing a mutation in amino acid 873 (R873X) that mimics the most COOH-terminal mutation known in PPH (Machado et al., 2001) (Fig. 1 A). This PPH mutant was chosen because it represents the smallest (minimal) deletion in the tail region of BMPR-II.

In immunoprecipitation experiments, the amount of BMPR-II (R873X) protein coimmunoprecipitated with LIMK1 was only 15% of the wild-type BMPR-II after adjustment for the level of expression of each protein (Fig. 3 B). These results suggest that the interaction between LIMK1 and all of the various mutated BMPR-II receptors present in PPH is likely to be diminished or abolished.

### The LIM domains of LIMK1 mediate the interaction with the tail of BMPR-II

To identify the region of LIMK1 mediating the interaction with BMPR-II, FLAG-tagged domains of LIMK1 (Fig. 3 C) were coexpressed with full-length BMPR-II in COS-7 cells. Cell lysates were incubated with FLAG M2 beads, and the bound proteins were analyzed by immunoblotting using an anti-BMPR-II antibody. BMPR-II interacted strongly with both full-length LIMK1 (Fig. 3 C, lane 9) and the LIM domains (lane 3), interacted weakly with the PDZ domain (lane 5), and did not interact with the kinase domain or the negative control, Btk (lanes 7 and 11). These results indicate that LIMK1 binds to BMPR-II primarily via its LIM domains, possibly with some contribution from the PDZ domain. The specificity of association between BMPR-II and the LIM domains of LIMK1 was further verified after coimmunoprecipitation analysis with overexpressed BMPR-II and the LIM domain protein LMO2 (Larson et al., 1996) where no interaction was observed (unpublished data). Although it is likely that the LIM domains of LIMK1 interact directly with the tail of BMPR-II, it is possible that this interaction is assisted by another protein such as a scaffolding protein or even actin. Previous yeast-two hybrid and mammalian cell interaction analyses have revealed that LIMK1 also interacts via its LIM domains with at least two other proteins, PKC (Kuroda et al., 1996) and the transmembrane ligand neuregulin (Wang et al., 1998). However, neither PKC nor neuregulin share any common sequence motifs with the 190-amino acid region of BMPR-II that binds LIMK1, and we were unable to identify any known protein binding motifs or recognizable functional domains within this 190-amino acid region.

### BMPR-II competes with PAK4 for interaction with LIMK1

PAK and ROCK activate LIMK1 after interaction with its LIM domains followed by phosphorylation of threonine 508. To examine whether BMPR-II could compete with PAK for the interaction with LIMK1, we performed copuri-

fication assays with LIMK1 and PAK4 in the presence and absence of overexpressed BMPR-II. GST-LIMK1, HA-PAK4, and BMPR-II were expressed separately in COS-7 cells. GST-LIMK1 was purified on glutathione-Sepharose beads, and 10 or 20  $\mu$ l of the beads containing purified LIMK1 was added to equal volumes of cell lysates of COS cells expressing either HA-PAK4, BMPR-II, or both. After washings, proteins that copurified with LIMK1 were detected by immunoblotting using anti-HA and anti-BMPR-II antibodies. As expected, both PAK4 and BMPR-II bind strongly to LIMK1 alone; however, in the presence of BMPR-II, the amount of PAK4 that copurified with LIMK1 was reduced by 2.86- and 2.3-fold for 10 and 20  $\mu$ l of GST-LIMK1, respectively (Fig. 3 D).

### BMPR-II is a negative regulator of LIMK1 activity

As endogenous LIMK1 and BMPR-II were found to associate, we examined if this interaction affected their known activities. To assess this, the ability of LIMK1 to phosphorylate cofilin using *in vitro* kinase assays in the presence or absence of BMPR-II was examined. Myc-tagged LIMK1 and myc-tagged BMPR-II were expressed separately in COS cells and then immunoprecipitated with anti-myc antibodies either alone or together after the lysates were combined. The immunocomplexes were labeled *in vitro* with [<sup>32</sup>P] $\gamma$ -ATP to determine their level of activity. Both kinase molecules exhibited high levels of autophosphorylation when assayed individually (Fig. 4 A). In addition, LIMK1, but not BMPR-II, was able to phosphorylate 5  $\mu$ g of recombinant GST-cofilin present in all samples (Fig. 4 A). However, when LIMK1 and BMPR-II were coimmunopurified, a decrease in the level of phosphorylated GST-cofilin was observed with no change evident in the level of phosphorylation of LIMK1 or BMPR-II. All samples were normalized for the amount of LIMK1 protein present, as determined by densitometry analysis of immunoblotted LIMK1. The level of GST-cofilin phosphorylation by LIMK1 was reduced up to five-fold after LIMK1 interaction with BMPR-II in six individual experiments performed where an average of  $0.45 \pm 0.10$  SEM was measured and compared with 1.0, the value given to the level of phosphorylated GST-cofilin in the presence of myc-tagged LIMK1 alone (Fig. 4 A). A reduction in GST-cofilin phosphorylation was confirmed in experiments where protein lysates containing FLAG-tagged or GFP-tagged LIMK1 proteins were combined with myc-tagged BMPR-II protein lysates and coimmunopurified using either anti-FLAG or anti-GFP antibodies, respectively (Fig. 4 B), and tested for their ability to phosphorylate cofilin. After normalization for LIMK1 protein, a reproducible decrease in the phosphorylation of GST-cofilin was evident (Fig. 4 B), as shown in Fig. 4 A. In addition, the activity of the LIMK1 kinase domain alone, as judged by its ability to phosphorylate cofilin, was not affected by the presence of BMPR-II (Fig. 4 B), indicating that the interaction between the two molecules leads to down-regulation of LIMK1 activity. Moreover, the presence of a tailless BMPR-II receptor did not affect the activity of LIMK1 (Fig. 4 C). The PPH-like mutant BMPR-II (R873X) did not affect the ability of LIMK1 to phosphorylate cofilin (unpublished data), supporting the notion that PPH mutations may compromise

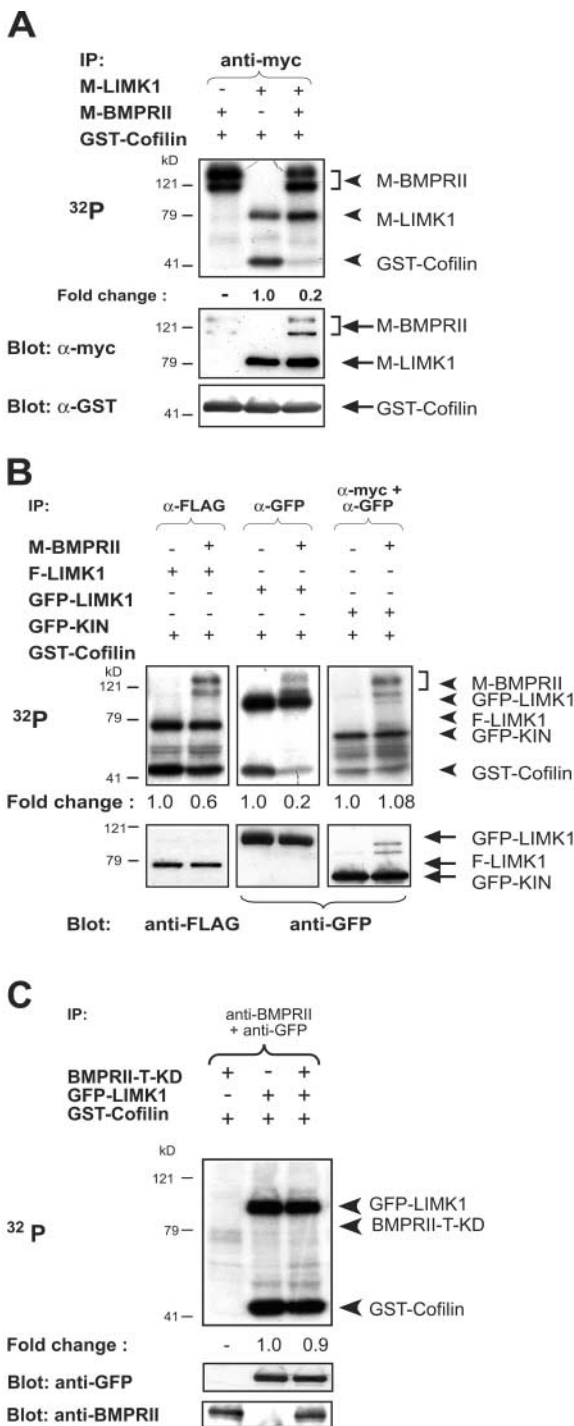


**Figure 4. Inhibition of LIMK1 function after interaction with BMPRII.** (A) *In vitro* kinase assay of coimmunoprecipitated myc-tagged LIMK1 and BMPRII (M-LIMK1 and M-BMPRII) proteins using 5  $\mu$ g of GST-cofilin as substrate. Autophosphorylated M-LIMK1 and M-BMPRII and phosphorylated GST-cofilin (arrowheads) and their level of expression as determined by immunoblotting (arrows) are indicated at the top and bottom panels, respectively. The level of cofilin phosphorylation is an indication of LIMK1 activity, and the fold change in cofilin phosphorylation was calculated by Phosphor-Image analysis after normalization for the level of LIMK1 expression as determined by immunoblotting. The level of cofilin phosphorylation in the presence of LIMK1 alone was used as the baseline and designated 1.0. (B) *In vitro* kinase assays of coimmunoprecipitated FLAG- or GFP-tagged LIMK1 (F- or GFP-LIMK1) or GFP-tagged kinase domain of LIMK1 (GFP-KIN) with or without M-BMPRII.

the regulation of LIMK1. Finally, in a separate set of experiments, the interaction of LIMK1 with BMPRII did not appear to alter the ability of BMPRII to phosphorylate BMPRII-A (unpublished data).

### BMP4 increases the activity of LIMK1

To demonstrate that the interaction between LIMK1 and BMPRII has biological significance, we studied the effect of BMP4 on the activity of LIMK1. As the only known substrate of LIMK1 is cofilin, change in the level of phospho-cofilin is a surrogate measure of LIMK1 activity. COS-7 cells were serum starved and then incubated in the presence or absence of 10 ng/ml BMP4 for periods of 5–30 min and compared with unstimulated cells. Cell lysates were subjected to immunoblotting with anti-phospho-cofilin antibodies. Western blot filters were subsequently stripped and reprobed with anti-cofilin antibodies to allow the absolute amount of cofilin to be measured. Incubation with BMP4 for 5 min resulted in a sevenfold increase in the level of phospho-cofilin compared with controls. An increased level of phospho-cofilin was maintained, but to a lesser extent after 10 and 30 min incubation with BMP4, relative to that found in untreated cells (Fig. 5 A).

We next examined the possibility that BMP4 also increases the activity of overexpressed LIMK1 in the presence of overexpressed BMPRII. COS-7 cells were transfected separately with GST-LIMK1 and both GST-LIMK1 and BMPRII. The cells were stimulated with 10 ng/ml BMP4 for 10 min, and lysates of stimulated and nonstimulated cells were subjected to immunoblot analysis using anti-phospho-cofilin and anti-cofilin antibodies. Expression of LIMK1 resulted in a 3.9-fold increase in the level of phospho-cofilin, in comparison with nontransfected cells (Fig. 5 B, lane 2). In the presence of BMP4, the level of phospho-cofilin in the LIMK1-expressing cells was increased 5.2-fold in comparison with nontransfected, nonstimulated cells (Fig. 5 B, lane 3). The level of phospho-cofilin in BMP4-stimulated LIMK1- and BMPRII-transfected cells was similar to that of LIMK1-transfected cells (Fig. 5 B, lane 5), indicating that BMP4 stimulation can overcome the inhibition of LIMK1 activity caused by BMPRII.

Given the effects that the interaction between LIMK1 and BMPRII has on LIMK1 activity, an obvious question that arises is whether BMPs can induce discernible short-term effects on the cells' cytoskeletal architecture. Therefore, we investigated the effects of BMP4 on the subcellular localization of endogenous LIMK1 and the arrangement of F-actin. Immunofluorescence analysis of unstimulated COS-7 cells demonstrated that endogenous LIMK1 predominantly resides in the cytosol with a perinuclear distribution. Lower levels of LIMK1 were also present at the plasma membrane at the leading edge of the cell where it colocalized with

(C) *In vitro* kinase assays of immunoprecipitated GFP-LIMK1 in the presence or absence of tailless kinase dead BMPRII (BMPRII-T-KD). 5  $\mu$ g of GST-cofilin is used as substrate in all samples. Phosphorylated proteins (arrowheads, top panel) and their level of expression after immunoblotting (arrows, bottom panel) are indicated. The fold change in GST-cofilin phosphorylation by LIMK1 was calculated as described above.

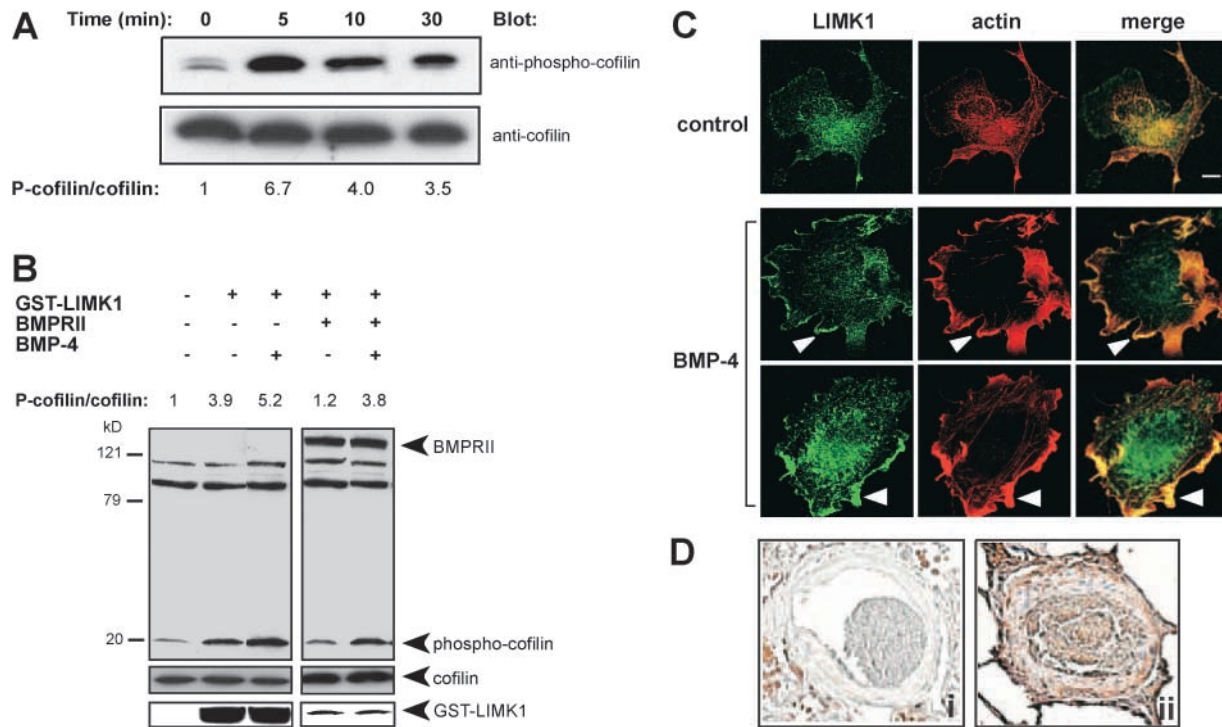


**Figure 5. Effects of BMP4 on LIMK1 activity and subcellular localization.** (A) Immunoblot of COS cell lysates before and after stimulation with 10 ng/ml BMP4. The membrane was probed with anti-phospho-cofilin, stripped, and re probed with anti-cofilin antibodies. The numbers below indicate the fold induction of phospho-cofilin level after BMP4 stimulation and were adjusted for the level of cofilin in the lysates. (B) Immunoblots of cell lysates prepared from COS cells overexpressing GST-LIMK1, BMPR-II, and both GST-LIMK1 and BMPR-II after or before BMP4 stimulation. The filters were probed with anti-BMPR-II (tail), anti-LIMK1 (rat monoclonal), anti-phospho-cofilin, and anti-cofilin antibodies. The numbers below indicate the fold induction of phospho-cofilin (P-cofilin) level after BMP4 stimulation and were adjusted for the level of cofilin in the lysates. The levels of overexpressed GST-LIMK1 and BMPR-II were consistently much higher when expressed separately than when coexpressed in the same cells. (C) Immunofluorescence analysis of endogenous LIMK1 and actin colocalization in unstimulated COS-7 cells (top) and in COS-7 cells stimulated with 100 ng/ml BMP4 for 10 min (middle and bottom). Arrowheads highlight the coredistribution of LIMK1 and F-actin to the cell's peripheral ruffles. Bar, 20  $\mu$ M. (D) Immunohistochemical analysis of endogenous LIMK1 expression in the precapillary pulmonary artery of normal human lung (i) and in lung tissue from an individual with PPH (ii).

F-actin (Fig. 5 C). However, after incubation with BMP4 for 10–30 min, changes to cell morphology and to the localization of LIMK1 and F-actin were observed. The cells flattened out and formed ruffles at their periphery, and in these regions, higher levels of LIMK1 and F-actin colocalization were now evident (Fig. 5 C).

**LIMK1 expression in pulmonary artery of PPH patient**

To further understand the effect of BMPR-II mutations on the possible LIMK1 involvement in the etiology of PPH, we performed immunohistochemical analysis of a tissue sample derived from a lung of an individual with PPH using an anti-LIMK1 antibody. This analysis revealed a high level of LIMK1 expression in the hyperproliferated smooth muscle cells of a precapillary pulmonary artery in comparison with an artery from a normal lung (Fig. 5 D).

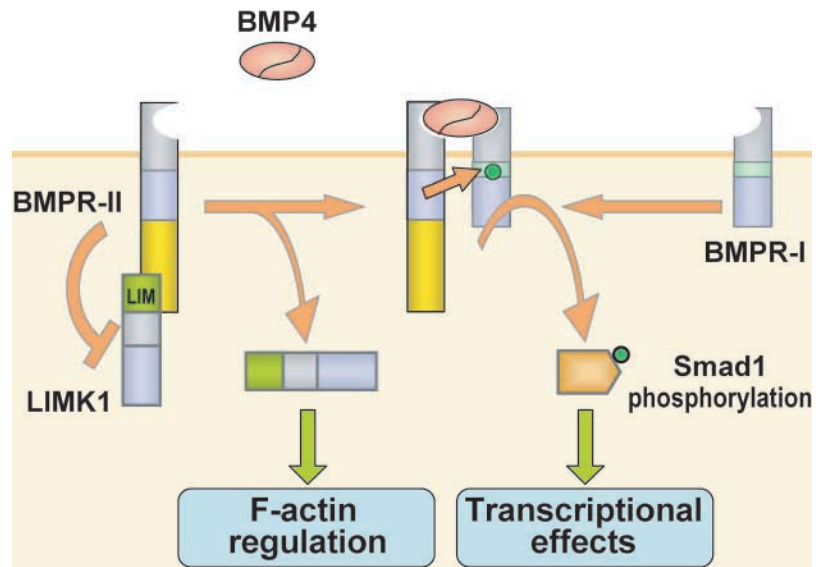
**Discussion**

The primary function of LIMK1 identified so far is to regulate actin dynamics by phosphorylating cofilin (Arber et al., 1998; Yang et al., 1998). We have shown that BMPR-II associates with LIMK proteins and subsequently reduces LIMK1's ability to phosphorylate cofilin, suggesting that

BMPR-II molecules negatively regulate the activity of LIMK1. How BMPR-II inhibits the activity of LIMK1 is not yet clear. It is possible that the binding of LIMK1 via its LIM domains to the tail of BMPR-II reduces its availability in the cytoplasm and limits its access to its activators PAK and ROCK, as we have demonstrated here for PAK4. Significantly, this inhibitory effect appears to be alleviated by BMP4 stimulation. It is possible that upon engagement of the BMP4 ligand by BMPR-II, followed by formation of BMP-BMPR-II-BMPR-IA complex, LIMK1 is dissociated from the BMPR-II tail, enabling it to more freely interact with other proteins, such as its activators, resulting in cofilin phosphorylation (Fig. 6).

After BMP4 stimulation of COS-7 cells, we observed a clear change in the subcellular localization of both LIMK1 and F-actin with an apparent increase in polymerized actin colocalized with LIMK1 at the cell periphery. BMPs are able to regulate a wide variety of morphogenetic processes during embryogenesis and in the adult (Hogan, 1996). BMP gradient concentrations are responsible for migration of cells during development. It is possible that the release of LIMK1 from the tail of BMPR-II alters the actin dynamics underlying cell motility. Moreover, it has been shown that BMP4 is involved in the activation of RhoB during neural crest devel-

**Figure 6. Schematic representation of two signaling outputs from the BMPR system.** In the canonical Smad signaling process, BMP4 binds to and brings together BMPR-I (-IA or -IB, also known as ALK3 and ALK6, respectively) and BMPR-II. BMPR-II phosphorylates the regulatory region (green box) of BMPR-I, activating the kinase domain (blue box), which phosphorylates Smad1, leading to its nuclear translocation for regulation of target genes. The present results show that the COOH-terminal tail domain (yellow box) of BMPR-II in the basal state binds to the LIM domain region of LIMK1 and inhibits LIMK1. BMP4 binding relieves this inhibitory interaction, enabling LIMK1 to phosphorylate cofilin, thereby regulating the actin cytoskeleton.



opment (Liu and Jessell, 1998), raising the possibility that BMP4 stimulation additionally activates LIMK1 by phosphorylation via the Rho/ROCK pathway.

The redistribution of actin filaments to the periphery of BMP-stimulated COS-7 cells is similar to that observed in adenocarcinoma cells stimulated by EGF (Chan et al., 2000). However, in the case of the EGF-stimulated cells, it was demonstrated that active cofilin is responsible for the newly formed actin filaments (Zebda et al., 2000), whereas in the present study, we observed increased levels of phosphorylated cofilin after BMP stimulation. Moreover, Zebda et al. (2000) have demonstrated that overexpression of the highly active kinase domain of LIMK1 completely inhibits the effects of EGF on actin polymerization. However, it is acknowledged that actin polymerization *in vivo* depends not only on severing of actin filaments by cofilin but also via other mechanisms, the combination of which appears cell type specific (for review see Condeelis, 2001). Thus, different combinations of factors may give rise to the similar actin polymerization phenotypes observed in BMP-stimulated COS-7 cells and EGF-stimulated adenocarcinoma cells.

BMPs bind to and activate BMPR-II, which in turn phosphorylates and activates BMPR-I, leading to the recruitment, phosphorylation, and subsequent nuclear translocation of a subset of Smad transcriptional regulators (Shi and Massague, 2003). Mutations affecting TGF $\beta$  signaling pathways in most other human disorders target Smad signaling (Massague et al., 2000). However, this is not the case in PPH because many of the *BMPRII* mutations target the tail domain of this receptor, which is dispensable for signaling via the Smad pathway (Eng, 2001; Nishihara et al., 2002). A prediction from our study is that these mutations would uncouple the activation of the Smad signaling pathway from the regulation of LIMK1 and actin dynamics. An important question that remains to be addressed is whether the BMPR-II kinase activity, which is also targeted by certain PPH mutations (Lane et al., 2000; Thomson et al., 2000; Machado et al., 2001), plays a role in LIMK1 inhibition.

Our preliminary analysis revealed that the level of LIMK1 protein in a precapillary pulmonary artery of an individual

with PPH is increased in the hyperproliferated smooth muscle cells in comparison with normal lung tissue. The increased level of LIMK1 in PPH pulmonary arteries could also correspond to increases in its activity. We propose that in PPH patients expressing tailless BMPR-II, LIMK1 activity is increased because it cannot be controlled by BMPR-II. Recent experiments in our laboratory suggest that the half-life of phosphorylated LIMK1 is much longer than that of the nonphosphorylated protein, and therefore we suspect that in PPH patients, the higher LIMK1 activity might translate directly into elevated protein levels. However, it remains to be determined if this dysregulation of LIMK activity could lead to the hyperproliferation of endothelial and smooth muscle cells characteristic of PPH.

In summary, the present findings provide a signaling function for the COOH-terminal tail domain of BMPR-II. This function is separate from Smad signaling via the associated type I receptors (Fig. 6). The transcriptional effects of BMPs and other TGF $\beta$  family members via the Smad pathway have been the subjects of extensive analysis, and their mechanistic basis is well understood (Hogan, 1996; Shi and Massague, 2003). However, much less is known about the molecular basis for the effects of BMP on cell morphology and migration. Our present results open the door for future investigation of the link between the BMPR system and the cytoskeleton via LIMK1.

## Materials and methods

### Yeast two-hybrid screens

LIMK1, Jun, and Lck bait cDNAs were subcloned into the yeast vector pGBT9. LIMK1 bait was used in yeast two-hybrid screens of mouse embryonic day 11 or human brain MATCHMAKER cDNA libraries (CLONTECH Laboratories, Inc.) according to the manufacturer's instructions.

### Constructs

cDNA clones isolated from LIMK1-interacting colonies were subcloned into the BamHI/XbaI restriction sites of the GFP expression vector pEGFP-C1 (CLONTECH Laboratories, Inc.). Untagged BMPR-II and HA-PAK4 were obtained from J. Rosenbaum (Procter & Gamble Pharmaceuticals, Mason, OH) and A. Minden (Columbia University, New York, NY), respectively. LIMK1 and BMPR-II full-length and truncated cDNAs were cloned into a modified, mammalian expression vector, pEF-BOS, encoding



either COOH- or NH<sub>2</sub>-terminal FLAG or myc epitope tags, respectively, and lacking the puromycin resistance gene and pGK promoter sequences (Huang et al., 1997).

### Generation and purification of anti-BMPR-II antibodies

A fragment of the human BMP type II receptor comprising amino acids 173–500, including the juxtamembrane and kinase domains, was produced as a recombinant His<sub>6</sub>-tagged polypeptide in *Escherichia coli* using pRSETA vector and purified using Talon metal affinity resin (CLONTECH Laboratories, Inc.) according to the manufacturer's protocol. A fragment consisting of amino acids 500–899, comprising the COOH-terminal extension of human BMPR-II, was expressed as a GST fusion protein in *E. coli* using pGEX4T1 vector. This fragment was purified as soluble protein using glutathione-Sepharose beads (Amersham Biosciences) according to the manufacturer's protocol and incubated with thrombin (final concentration 10 U/ml) overnight at 4°C to release the polypeptide from the GST tag. The cleaved polypeptide was resolved by SDS-polyacrylamide gels and cut out of the gel. These proteins were coupled to CNBr-activated Sepharose (Amersham Biosciences) and used to raise antibodies in rabbits. Antisera were affinity purified using columns packed with these immunogen-conjugated Sepharose following standard protocols (Harlow and Lane, 1999).

### Transfection, immunoprecipitation, and immunoblotting analysis

COS-7 cells were electroporated with cDNA constructs using a standard procedure and grown in DME/10% FCS for 48 h before lysing in a PBS buffer containing 50 mM Tris-HCl (pH 7.4), 150 mM NaCl, 1% Triton X-100, and a cocktail of protease inhibitors (Roche). Lysates were combined for coimmunoprecipitation analyses essentially as previously described (Bernard et al., 1994) but using the lysis buffer for the wash buffer. Immunoprecipitated proteins or whole lysates were separated on SDS-polyacrylamide minigels (Invitrogen) followed by transferring to Hybond-C nitrocellulose filters (Amersham Biosciences). Filters were probed with the following antibodies at the following dilutions: rabbit anti-BMPR-II juxtamembrane polyclonal antibodies, 1:1,000 (provided by J. Rosenbaum); rabbit anti-phospho-cofilin polyclonal antibodies, 1:1,000 (provided by J. Bamberg, Colorado State University, Fort Collins, CO); rabbit anti-cofilin polyclonal antibodies, 1:5,000 (provided by J. Bamberg); rabbit anti-GST polyclonal antibodies, 1:4,000 (AMRAD); rabbit anti-GFP polyclonal antibodies, 1:3,000 (Molecular Probes); mouse anti-FLAG M2 monoclonal antibody, 1:10,000 (Sigma-Aldrich); and mouse anti-myc antibody monoclonal, 1:6,000 (Zymed Laboratories). Bound primary antibodies were visualized with the horseradish peroxidase-conjugated secondary antibodies, goat anti-mouse, goat anti-rat, or goat anti-rabbit IgG (Silenus). To detect the interaction between endogenous BMPR-II and LIMK1, NIH3T3 cells were lysed in buffer containing 50 mM Tris (pH 8.0), 150 mM NaCl, 10 mM NaF, 10 mM β-glycerolphosphate, 10% glycerol, 0.5% NP-40, 1 mM DTT, and a cocktail of protease inhibitors (Roche). Immunoprecipitations were performed as previously described (Chen et al., 2002). The following antibody dilutions were used: 1:500 for mouse anti-LIMK1 (BD Biosciences) and 1:1,000 for rabbit anti-BMPR-II (tail and kinase).

### GST and FLAG affinity purification

Cell lysates containing overexpressed GST- or FLAG-tagged proteins were incubated with glutathione-Sepharose beads (Amersham Biosciences) or with anti-FLAG M2 beads (Sigma-Aldrich), respectively. Bound FLAG-tagged proteins were eluted with 100 μg/ml FLAG peptide (Sigma-Aldrich), and GST-tagged proteins were released after boiling for 5 min.

### In vitro kinase assays

Electroporated COS-7 cells were lysed in PBS containing 20 mM Hepes (pH 7.4), 150 mM KCl, 0.1% Triton X-100, protease inhibitors, 10 mM NaF, 1 mM Na<sub>3</sub>VO<sub>4</sub>, and 10 mM NaP<sub>2</sub>O<sub>7</sub> and sonicated for 10 s. Immunopurified proteins were subjected to an in vitro kinase assay and recovered using ProbeQuant G-50 microcolumns (Amersham Biosciences). These columns increase reproducibility and protein recovery of immunoprecipitated protein complexed (Brymore et al., 2001). In brief, the ProbeQuant G-50 beads were removed, and the protein-antibody-coupled Sepharose beads were pipetted into the column. Under vacuum aspiration, the samples were washed three times in 1 ml of the Hepes lysis buffer and twice with the in vitro kinase assay buffer (20 mM Hepes, pH 7.4, 150 mM MgCl<sub>2</sub>, 10 mM MnCl<sub>2</sub>, 10 mM NaF, and 1 mM Na<sub>3</sub>VO<sub>4</sub> in PBS). The in vitro kinase assay was performed as previously described (Arber et al., 1998). To elute the phosphorylated bound protein complexes, the columns were capped, boiled for 5 min in 1.5-ml microtubes, and the protein-antibody complexes were collected from the columns by centrifugation. After electrophoresis and Western blotting, phosphorylated proteins were de-

tected and quantitated using a PhosphorImager (400 series; Molecular Dynamics). The loading of proteins was determined after immunoblotting and densitometry analysis.

### Expression of endogenous LIMK1 in COS-7 cells and tissue sections

COS-7 cells (5 × 10<sup>3</sup>) were plated on fibronectin-treated coverslips in a 24-well plate and incubated with DME containing 10% FCS for 24 h. The cells were washed with PBS and incubated for 4 h with DME before addition of BMP4 (R&D Systems) (100 ng/ml) for 1, 5, 10, 30, and 60 min. The cells were fixed with 1% paraformaldehyde, washed with PBS, and permeabilized for 1 h with PBS containing 2% normal goat serum, 5% FCS, and 0.1% Tween-20. Endogenous LIMK1 expression was detected using a rat anti-LIMK1 monoclonal antibody (Yoshioka et al., 2003) at a 1:500 dilution followed by Alexa<sup>®</sup>488 anti-rat IgG (1:7,500; Molecular Probes). F-actin was stained with TRITC-phalloidin (Molecular Probes). The coverslips were mounted using antifade mounting medium (DakoCytomation) and visualized by confocal microscopy. Paraffin-embedded tissue sections were treated and stained as previously described (O'Reilly et al., 1998) with the rat anti-LIMK1 monoclonal antibody (1:100 dilution).

### BMP4 stimulation of COS cells

COS cells (10<sup>4</sup>) were plated onto 6-cm dishes, and 24 h later, they were washed three times with PBS and serum starved for 4 h in DME before addition of 10 ng/ml BMP4 (R&D Systems) diluted in 0.1% BSA in PBS for 5–30 min. Control plates were incubated for the same time periods in 0.1% BSA in PBS. Cells were lysed in lysis buffer and were subjected to Western blot analysis as described above.

We thank Drs. J. Rosenbaum, N. Nosworthy (University of Sydney, Sydney, Australia), and J. Bamberg for their gifts of the mouse BMPR-II cDNA, rabbit polyclonal anti-BMPR-II (juxtamembrane), recombinant GST-cofilin, and anti-phospho-cofilin and cofilin antibodies, respectively. We thank Drs. C.A. Stanyon (Wayne State University School of Medicine, Detroit, MI) and W.C. Nichols (Vanderbilt University Medical Center, Nashville, TN) for help in the yeast two-hybrid screens and for the PPH lung tissue, respectively.

This work was supported by the Australian National Health and Medical Research Council (O. Bernard) and by National Institutes of Health grant CA34610 (J. Massague).

Submitted: 10 December 2002

Accepted: 18 July 2003

## References

- Aberle, H., A.P. Haghghi, R.D. Fetter, B.D. McCabe, T.R. Magalhaes, and C.S. Goodman. 2002. Wishful thinking encodes a BMP type II receptor that regulates synaptic growth in *Drosophila*. *Neuron*. 33:545–558.
- Allan, D.W., S.E. Pierre, I. Miguel-Aliaga, and S. Thor. 2003. Specification of neuroepithelial cell identity by the integration of retrograde BMP signaling and a combinatorial transcription factor code. *Cell*. 113:73–86.
- Arber, S., F.A. Barbayannis, H. Hanser, C. Schneider, C.A. Stanyon, O. Bernard, and P. Caroni. 1998. Regulation of actin dynamics through phosphorylation of cofilin by LIM-kinase. *Nature*. 393:805–809.
- Bernard, O., S. Ganiatsas, G. Kannourakis, and R. Dringen. 1994. Kiz-1, a protein with LIM zinc finger and kinase domains, is expressed mainly in neurons. *Cell Growth Differ.* 5:1159–1171.
- Birkenfeld, J., H. Betz, and D. Roth. 2003. Identification of cofilin and LIM-domain-containing protein kinase 1 as novel interaction partners of 14-3-3 ζ. *Biochem. J.* 369:45–54.
- Brymore, A., M.A. Cousin, B.D. Roufogalis, and P.J. Robinson. 2001. Enhanced protein recovery and reproducibility from pull-down assays and immunoprecipitations using spin columns. *Anal. Biochem.* 295:119–122.
- Chan, A.Y., M. Bailly, N. Zebda, J.E. Segall, and J.S. Condeelis. 2000. Role of cofilin in epidermal growth factor-stimulated actin polymerization and lamellipod protrusion. *J. Cell Biol.* 148:531–542.
- Chen, C.R., Y. Kang, P.M. Siegel, and J. Massague. 2002. E2F4/5 and p107 as Smad cofactors linking the TGFβ receptor to c-myc repression. *Cell*. 110: 19–32.
- Condeelis, J. 2001. How is actin polymerization nucleated in vivo? *Trends Cell Biol.* 11:288–293.
- Dan, C., A. Kelly, O. Bernard, and A. Minden. 2001. Cytoskeletal changes regulated by the PAK4 serine/threonine kinase are mediated by LIM kinase 1

- and cofilin. *J. Biol. Chem.* 276:32115–32121.
- Edwards, D.C., L.C. Sanders, G.M. Bokoch, and G.N. Gill. 1999. Activation of LIM-kinase by Pak1 couples Rac/Cdc42 GTPase signalling to actin cytoskeletal dynamics. *Nat. Cell Biol.* 1:253–259.
- Eng, C. 2001. To be or not to BMP. *Nat. Genet.* 28:105–107.
- Fields, S., and O. Song. 1989. A novel genetic system to detect protein-protein interactions. *Nature.* 340:245–246.
- Gohla, A., and G.M. Bokoch. 2002. 14-3-3 regulates actin dynamics by stabilizing phosphorylated cofilin. *Curr. Biol.* 12:1704–1710.
- Harlow, E., and P. Lane. 1999. Using Antibodies. Cold Spring Harbor Laboratory, Cold Spring Harbor, NY. 495 pp.
- Hogan, B.L. 1996. Bone morphogenetic proteins: multifunctional regulators of vertebrate development. *Genes Dev.* 10:1580–1594.
- Huang, D.C., S. Cory, and A. Strasser. 1997. Bcl-2, Bcl-XL and adenovirus protein E1B19kD are functionally equivalent in their ability to inhibit cell death. *Oncogene.* 14:405–414.
- Kuroda, S., C. Tokunaga, Y. Kiyohara, O. Higuchi, H. Konishi, K. Mizuno, G.N. Gill, and U. Kikkawa. 1996. Protein-protein interaction of zinc finger LIM domains with protein kinase C. *J. Biol. Chem.* 271:31029–31032.
- Lane, K.B., R.D. Machado, M.W. Pauciulo, J.R. Thomson, J.A. Phillips, III, J.E. Loyd, W.C. Nichols, and R.C. Trembath. 2000. Heterozygous germline mutations in BMPR2, encoding a TGF- $\beta$  receptor, cause familial primary pulmonary hypertension. The International PPH Consortium. *Nat. Genet.* 26:81–84.
- Larson, R.C., I. Lavenir, T.A. Larson, R. Baer, A.J. Warren, I. Wadman, K. Nottage, and T.H. Rabbitts. 1996. Protein dimerization between Lmo2 (Rbtn2) and Tal1 alters thymocyte development and potentiates T cell tumorigenesis in transgenic mice. *EMBO J.* 15:1021–1027.
- Liu, F., F. Ventura, J. Doody, and J. Massague. 1995. Human type II receptor for bone morphogenic proteins (BMPs): extension of the two-kinase receptor model to the BMPs. *Mol. Cell. Biol.* 15:3479–3486.
- Liu, J.P., and T.M. Jessell. 1998. A role for rhoB in the delamination of neural crest cells from the dorsal neural tube. *Development.* 125:5055–5067.
- Machado, R.D., M.W. Pauciulo, J.R. Thomson, K.B. Lane, N.V. Morgan, L. Wheeler, J.A. Phillips, III, J. Newman, D. Williams, N. Galie, et al. 2001. BMPR2 haploinsufficiency as the inherited molecular mechanism for primary pulmonary hypertension. *Am. J. Hum. Genet.* 68:92–102.
- Maekawa, M., T. Ishizaki, S. Boku, N. Watanabe, A. Fujita, A. Iwamatsu, T. Obinata, K. Ohashi, K. Mizuno, and S. Narumiya. 1999. Signaling from Rho to the actin cytoskeleton through protein kinases ROCK and LIM-kinase. *Science.* 285:895–898.
- Massague, J., S.W. Blain, and R.S. Lo. 2000. TGF $\beta$  signaling in growth control, cancer, and heritable disorders. *Cell.* 103:295–309.
- Morrell, N.W., X. Yang, P.D. Upton, K.B. Jourdan, N. Morgan, K.K. Sheares, and R.C. Trembath. 2001. Altered growth responses of pulmonary artery smooth muscle cells from patients with primary pulmonary hypertension to transforming growth factor- $\beta$ 1 and bone morphogenetic proteins. *Circulation.* 104:790–795.
- Nishihara, A., T. Watabe, T. Imamura, and K. Miyazono. 2002. Functional heterogeneity of bone morphogenetic protein receptor-II mutants found in patients with primary pulmonary hypertension. *Mol. Biol. Cell.* 13:3055–3063.
- O'Reilly, L.A., L. Cullen, K. Moriishi, L. O'Connor, D.C. Huang, and A. Strasser. 1998. Rapid hybridoma screening method for the identification of monoclonal antibodies to low-abundance cytoplasmic proteins. *Biotechniques.* 25: 824–830.
- Shi, Y., and J. Massague. 2003. Mechanisms of TGF- $\beta$  signaling from cell membrane to the nucleus. *Cell.* 113:685–700.
- Thomson, J.R., R.D. Machado, M.W. Pauciulo, N.V. Morgan, M. Humbert, G.C. Elliott, K. Ward, M. Yacoub, G. Mikhail, P. Rogers, et al. 2000. Sporadic primary pulmonary hypertension is associated with germline mutations of the gene encoding BMPR-II, a receptor member of the TGF- $\beta$  family. *J. Med. Genet.* 37:741–745.
- Wang, J.Y., K.E. Frenzel, D. Wen, and D.L. Falls. 1998. Transmembrane neuregulins interact with LIM kinase 1, a cytoplasmic protein kinase implicated in development of visuospatial cognition. *J. Biol. Chem.* 273:20525–20534.
- Wieser, R., L. Attisano, J.L. Wrana, and J. Massague. 1993. Signaling activity of transforming growth factor  $\beta$  type II receptors lacking specific domains in the cytoplasmic region. *Mol. Cell. Biol.* 13:7239–7247.
- Yang, N., O. Higuchi, K. Ohashi, K. Nagata, A. Wada, K. Kangawa, E. Nishidi, and K. Mizuno. 1998. Cofilin phosphorylation by LIM-kinase 1 and its role in Rac-mediated actin reorganization. *Nature.* 393:809–812.
- Yoshioka, K., V. Foletta, O. Bernard, and K. Itoh. 2003. A role for LIM kinase in cancer invasion. *Proc. Natl. Acad. Sci. USA.* 100:7247–7252.
- Zebda, N., O. Bernard, M. Bailly, S. Welti, D.S. Lawrence, and J.S. Condeelis. 2000. Phosphorylation of ADF/cofilin abolishes EGF-induced actin nucleation at the leading edge and subsequent lamellipod extension. *J. Cell Biol.* 151:1119–1128.



Minerva Access is the Institutional Repository of The University of Melbourne

**Author/s:**

Foletta, VC; Lim, MA; Soosairaiyah, J; Kelly, AP; Stanley, EG; Shannon, M; He, W; Das, S; Massague, J; Bernard, O

**Title:**

Direct signaling by the BMP type II receptor via the cytoskeletal regulator LIMK1

**Date:**

2003-09-15

**Citation:**

Foletta, V. C., Lim, M. A., Soosairaiyah, J., Kelly, A. P., Stanley, E. G., Shannon, M., He, W., Das, S., Massague, J. & Bernard, O. (2003). Direct signaling by the BMP type II receptor via the cytoskeletal regulator LIMK1. *JOURNAL OF CELL BIOLOGY*, 162 (6), pp.1089-1098.  
<https://doi.org/10.1083/jcb.200212060>.

**Persistent Link:**

<http://hdl.handle.net/11343/256757>

**File Description:**

published version

**License:**

CC BY-NC-SA